Detection of Initial Stage of Aluminum Corrosion in NaCl Solution Utilizing Surface Plasmon Resonance

Terukazu Kosako, Munehiro Nishida, and Yutaka Kadoya, *Member, IEEE*

***Abstract*—Surface plasmon resonance (SPR) spectra on Al films in the Kretschmann configuration is investigated aiming at the rapid detection of the Al corrosion in NaCl solution. The angle of the dip, occurred in the SPR spectra, was observed to decrease in the first 20 min and then increase with the increase of the immersion time. Calculations based on a simple multilayer model suggest that the observed initial decrease and the subsequent increase in the dip angle correspond to the thinning of the oxide layer and that of Al, respectively. The model also explains the observed deepening of the dip. The decrease in the effective Al thickness is estimated to be about 10 nm after the immersion in 3 wt% NaCl solution for 20 hours, though the quantitative discussion becomes difficult for longer immersion time. The corrosion is surely detectable for the change smaller than 5 nm in the effective Al thickness corresponding to the immersion time of 2 hours. The results indicate that the SPR-based method is promising for detecting the initial stage of Al corrosion in nanoscale.**

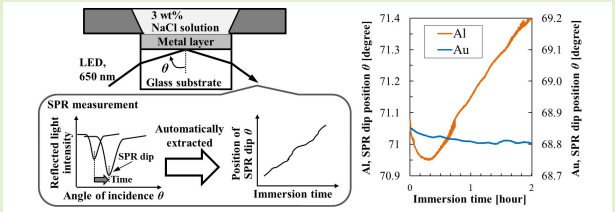

Surface plasmon resonance (SPR) measurement utilizing Kretschmann configuration is used to demonstrate the detection of corrosion of Al in 3 wt% NaCl solution. Comparison with the case of Au suggesting the possibility that corrosion of Al is detected. Since the Au is chemically stable to NaCl solution, and its variation is obviously smaller than that of Al.

***Index Terms*—Surface plasmon resonance, optical sensor, aluminum film, corrosion.**

I. Introduction

SURFACE plasmon resonance (SPR) occurring at the interface between a metal and the surrounding medium has been utilized for sensors [1]–[3], because of its sensitivity to the variation of the surrounding medium. Most of these sensors utilize attenuated total reflection (ATR) in the Kretschmann configuration [4], in which a thin metal film deposited on a prism surface is irradiated by a *p*-polarized plane wave through the prism, and the reflectance is measured as a function of the wavelength or incident angle. Usually, the dip position in the trace is analyzed since it depends quite sensitively on the permittivity of the surrounding medium, the glass substrate (prism), and the metal film itself. Although recent papers have revealed that the spectral shape around the dip originates from a type of Fano resonance and hence the dip position does not exactly indicate the SPR condition in practical systems [5], [6], we call the dip in the reflectance the SPR dip for simplicity in this paper.

Because of its chemical stability, Au has been widely used as the metal film in SPR-based sensors. Other metals have also been investigated with the aim of using SPR in a wider spectral range as well as to reduce the material cost of commercial SPR-based sensors [7]–[9]. However, when using metals with low chemical stability, the effects of the corrosion of the metal film on the measurement result should be taken into account. Bussjager and Macleod have demonstrated that the deposition of a thin copper layer of approximately 1 nm thickness improves the corrosion resistance of Ag to laboratory air, air with a relative humidity of 94% in a test chamber, and aqueous H_2O [10]. From the viewpoint of biosensing applications, Oliveira *et al.* [11] have evaluated the corrosion resistance of an Al film in an aqueous solution. They reported that a hydrous form likely coexists with the Al oxide film and remains stable in a deionized water solution. In contrast, they reported that Al corrodes in phosphate-buffered saline (PBS) containing substances such as Cl^- and PO_4^{-3} that are corrosive to Al. They also showed theoretically that the shape of the SPR dip changes as the Al film thickness decreases with the adoption of a multilayer model. These previous works, as Bussjager and Macleod mentioned [10], have suggested the possibility that SPR measurement can be used as a sensitive method for the detection of metal corrosion itself.

Manuscript received February 20, 2020; revised April 3, 2020; accepted April 3, 2020. Date of publication April 10, 2020; date of current version July 17, 2020. The associate editor coordinating the review of this article and approving it for publication was Dr. Carlos Marques. *(Corresponding author: Terukazu Kosako.)*

Terukazu Kosako is with the Yazaki Research and Technology Center, YAZAKI Corporation, Shizuoka 410-1194, Japan (e-mail: terukazu.kosako@jp.yazaki.com).

Munehiro Nishida and Yutaka Kadoya are with the Graduate School of Advanced Science and Engineering, Hiroshima University, Higashihiroshima 739-8530, Japan (e-mail: mnishida@hiroshima-u.ac.jp;kd@hiroshima-u.ac.jp).

Digital Object Identifier 10.1109/JSEN.2020.2987007

On the other hand, in the automotive industry, the need to reduce greenhouse gas emission has led to the increased adoption of Al and its alloys for automotive parts, including the body structure and wires, so as to reduce the vehicle weight and increase fuel efficiency. Although Al exhibits corrosion resistance under a dry atmosphere since a protective natural oxide film is promptly formed on the Al surface, Al corrodes in highly humid and corrosive environments [12, p. 297], [13, p. 272]–[17, p. 243]. A major cause of the corrosion of Al is the chloride ions mainly derived from airborne sea salt [17, p. 254]. In marine areas, the corrosion rate of Al is 0.4–0.6 μm/year [13, p. 273]. Therefore, there is an increasing need to measure the corrosion of Al. However, the conventional corrosion measurement of Al and its alloys, in which the mass loss is measured by microgravimetry, takes a time as long as a few months [13, p. 145], [17, pp. 168–173]. In this work, we investigated SPR-based sensing as a rapid but reliable method of detecting the corrosion of Al. We show that it is possible to measure a corrosion-induced reduction in Al thickness as small as 5 nm in 3 wt% NaCl solution, which is a practically important solution with salinity equivalent to the seawater concentration.

II. Experiments

Figure 1 shows a schematic diagram of the experimental system utilized in this work. We used a commercial equipment (OPTOQUEST SPR-01), which adopts the focused light ATR method based on the Kretschmann configuration [18] with a 650 nm LED. The p-polarized light is focused at a metal film through a glass substrate, and the reflected light is detected by a CMOS image sensor. Since the incident beam is composed of beams with different incident angles, the angular distribution of the reflected light is measured at a single time. The angle-dependent reflectance, which we call reflectance spectrum, is monitored and the extraction of the SPR dip position is performed at every 3 s by the software dedicated to the system. NaCl solution of 3 wt% concentration is fed to the metal surface in a flow system as shown in Fig. 1 to suppress the compositional change and the inhomogeneity of the solution. The flow speed was 30 μl/min. Before the solution is fed, the surface of the metal film is exposed to air, for which a SPR dip is not observed in the CMOS image, because it is out of the measurable angle range of the used equipment. When the solution reaches the metal surface, a dip suddenly appears in the image. Hence, we define the time zero (the arrival of the solution at the metal surface) by the appearance of the SPR dip.

Figure 2(a) shows the design of the Au film sample provided by OPTOQUEST and used in this study as a reference. An Au film of 48 nm thickness was deposited on a BK7 substrate (area: 3 mm × 5 mm, thickness: 2 mm). Figure 2(b) shows the design of the Al film samples purchased from SIGMAKOKI. Al films were deposited on a synthetic quartz substrate (the same size as that for the Au sample) using a vacuum coating equipment. The thicknesses of Al used in this work were about 21 nm with an error of nm order, which were measured by transmission electron microscopy (TEM). The air-formed natural oxide film on Al consists entirely of

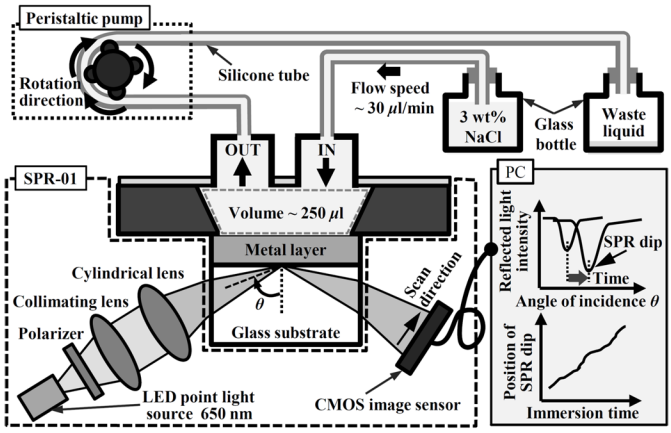

Fig. 1. Measurement system used in this work. The 3 wt% NaCl solution was fed to the metal surface by a flow system to stabilize the composition and homogeneity of the solution. The measurement was performed with SPR-01 (OPTOQUEST) controlled by a dedicated software on a personal computer (PC).

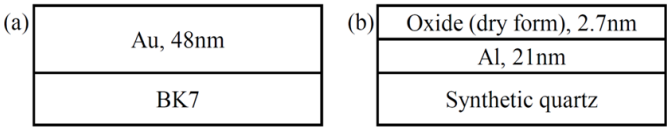

Fig. 2. Samples used in this work. (a) Au film of 48 nm thickness on a BK7 substrate. (b) Al film of about 21 nm thickness on synthetic quartz substrate. The measured thickness of the oxide layer in a dry form (consists entirely of Al_2O_3) was about 2.7 nm.

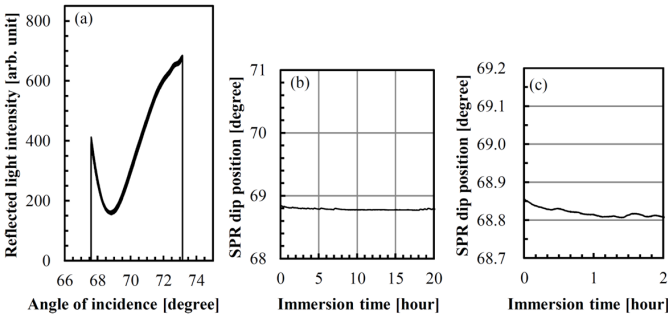

Fig. 3. Results of the SPR measurement for the Au film in 3 wt% NaCl solution. (a) Reflectance spectra recorded with one hour interval during 20-hour immersion. (b) Position of SPR dip as a function of immersion time extracted from the spectra as shown in (a). (c) Enlarged view of (b).

Al_2O_3 [12, p. 231]. The thickness of the natural oxide in a dry form was estimated to be about 2.7 nm by angle-resolved X-ray photoelectron spectroscopy (XPS) [19]–[22]. Here, the natural oxide is likely to be amorphous [11], [12, p. 235], [13, p. 144], [14], [17, pp. 102–105]. As mentioned later, the oxide film thickness may increase upon contact with the aqueous solution [11]. The samples used in the TEM and XPS measurements were fabricated by the same procedure as the samples used in the SPR measurement.

Figure 3 shows the results obtained with the Au film sample. Figure 3(a) shows the reflectance spectra recorded at every one hour during 20-hour immersion. All traces are almost the same. Figure 3(b) shows the angle of the SPR dip extracted from the spectra as shown in Fig. 3(a) as a function of

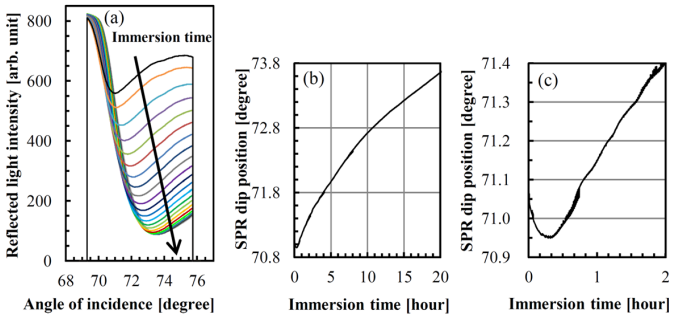

Fig. 4. Results of the SPR measurement for the Al film sample with initial thickness of about 21 nm. (a) Reflectance spectra recorded with one hour interval during 20-hour immersion. (b) Position of SPR dip as a function of immersion time extracted from the reflectance spectra as shown in (a). (c) Enlarged view of (b).

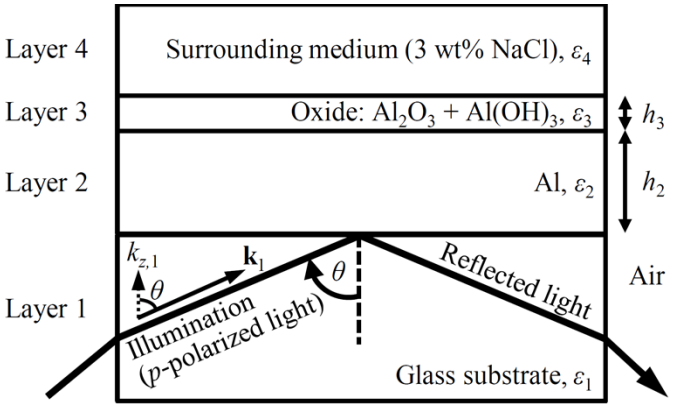

Fig. 5. Four-layer model used in this work. It consists of (i) a synthetic quartz substrate ($n_1 = 1.457$ at 650 nm [24]), (ii) an Al film ($n_2 = 1.5724 + i7.7354$ at 652 nm [25], thickness h_2), (iii) an oxide layer (ε_3, thickness h_3) composed of Al_2O_3 ($n_{oxide} = 1.6764$ at 650 nm [27], [28]) and $Al(OH)_3$ ($n_{hydroxide} = 1.57$ [29]), and (iv) 3 wt% NaCl solution [$n_4 = 1.3380$, measured by a refractometer (ATAGO PAL-RI)].

the immersion time. Figure 3(c) shows the enlarged view of Fig. 3(b). One can see a slight shift of the SPR dip to a lower angle for the immersion up to 1 hour, which is likely to be a time for the stabilization of the solution flow. However, the variation of the SPR dip position is negligible after it, which demonstrates that the Au film and the solution flow are both very stable.

Figure 4 shows the results for the Al film sample. Figure 4(a) shows the reflectance spectra recorded at every one hour during 20-hour immersion. Figure 4(b) shows the position of the SPR dip as a function of the immersion time extracted from the reflectance spectra as shown in Fig. 4(a). Figure 4(c) shows the enlarged view of Fig. 4(b). A shift of the SPR dip to a lower angle is observed in the initial 20 min as in the Au case. But the shift is larger than that in Au, implying that a change in the Al film or in the oxide layer occurs in addition to the flow stabilization. After the initial decrease, in contrast to the Au case, the SPR dip position definitely shifts to a higher angle with increasing immersion time, indicating clearly that a change in the sample, namely the corrosion, occurs in the Al sample. In other words, the SPR measurement can detect the Al corrosion in the NaCl environment in the time as short as a few hours.

III. Evaluation of the Corrosion Depth

Details of the initial corrosion process of Al in the presence of chloride ions, particularly the role and the change of the oxide layer, are not well understood. Qualitatively, however, it has been shown from various experimental results that there are three coexisting mechanisms: (i) a penetration mechanism, (ii) a film thinning mechanism, and (iii) a film rupture mechanism [12, p. 283], [15]. In all the models, the chloride ions are considered to penetrate through the oxide overlayer and facilitate the electrochemical dissolution of the underlying Al at the oxide/Al interface. On the other hand, according to the film thinning mechanism, the oxide layer also suffers from dissolution. The thinning of the oxide layer is, however, compensated by the oxidation of Al at the oxide/Al interface by the oxygen ions generated by the electrons created during the electrochemical dissolution of Al, which permeate through the oxide layer. Therefore, the models imply that the thickness of the oxide layer initially decreases and then becomes reasonably constant while the dissolution of Al continues. In practice, however, the reaction does not proceed uniformly in the plane since the penetration of the chloride ions occurs preferentially at various defects. In addition, the dissolution at the oxide/Al interface produces blisters and cracks in the oxide layer. As a result, the corrosion involves pits randomly distributed on the surface and is called pitting corrosion [12, p. 297].

Although the effect of such pits cannot be taken into account, a simple flat multilayer model has been used to describe the SPR measurement of Al films successfully [11], [23]. Such a simplification may be allowed for the very initial stage of the corrosion, in which the roughening of the surface by pitting corrosion is not severe and each layer can be modeled as a flat layer with an effective thickness and the refractive index of the original material. Here, we analyze the above experimental results using a flat four-layer model with effective thicknesses.

Figure 5 shows the four-layer model used in this work. The model consists of (i) a synthetic quartz substrate with refractive index $n_1 = 1.457$ at 650 nm [24], (ii) an Al film with refractive index $n_2 = 1.5724 + i7.7354$ at 652 nm [25] and a thickness of h_2, (iii) an oxide layer with refractive index n_3 and a thickness of h_3, and (iv) 3 wt% NaCl solution with refractive index $n_4 = 1.3380$, measured by a refractometer (ATAGO PAL-RI).

As for the oxide layer, we need to consider the distension in aqueous solution [11], [26]. In air, the oxide layer can be regarded as Al_2O_3 [12, p. 230] and the thickness is 2.7 nm in our sample as mentioned above. In the aqueous solution, however, the oxide layer may contain $Al(OH)_3$, since Al reacts readily with aqueous solution to form hydroxide [12, p. 230], [26]. Therefore, we estimated the relative permittivity of the oxide layer of thickness h_3 using the Maxwell-Garnett model [23],

$$\varepsilon_3 = \varepsilon_{\text{oxide}} \frac{(1+2f_0)\,\varepsilon_{\text{hydroxide}} + 2(1-f_0)\,\varepsilon_{\text{oxide}}}{(1-f_0)\,\varepsilon_{\text{hydroxide}} + (f_0+2)\,\varepsilon_{\text{oxide}}}. \quad (1)$$

Here, $\varepsilon_{\text{oxide}}$ and $\varepsilon_{\text{hydroxide}}$ are the relative permittivity of Al_2O_3 and $Al(OH)_3$, respectively, and the volume fraction of the $Al(OH)_3$ is calculated as $f_0 = (h_3 - 2.7)/h_3$. The values of the relative permittivity, $\varepsilon_{\text{oxide}} = n^2_{\text{oxide}}$ and $\varepsilon_{\text{hydroxide}} = n^2_{\text{hydroxide}}$, were calculated using the literature values $n_{\text{oxide}} = 1.6764$ at 650 nm [27], [28] and $n_{\text{hydroxide}} = 1.57$ [29], respectively.

In the case of p-polarized incident light of wavelength in vacuum λ_0, the reflectance R is given by the following expression (2) [23].

$$R = \left| \frac{\begin{array}{l} r_{12}\left[1 + r_{23}r_{34}exp\left(2ik_{z3}h_3\right)\right] \\ +\left[r_{23} + r_{34}exp\left(2ik_{z3}h_3\right)\right]exp\left(2ik_{z2}h_2\right) \end{array}}{\begin{array}{l} 1 + r_{23}r_{34}exp\left(2ik_{z3}h_3\right) \\ +r_{12}\left[r_{23} + r_{34}exp\left(2ik_{z3}h_3\right)\right]exp\left(2ik_{z2}h_2\right) \end{array}} \right|^2, \quad (2)$$

$$r_{i,i+1} = \frac{\frac{k_{z,i}}{\varepsilon_i} - \frac{k_{z,i+1}}{\varepsilon_{i+1}}}{\frac{k_{z,i}}{\varepsilon_i} + \frac{k_{z,i+1}}{\varepsilon_{i+1}}}, \quad (3)$$

$$k_{z,i} = \frac{2\pi}{\lambda_0}\sqrt{\varepsilon_i - \varepsilon_1 sin^2\theta}. \quad (4)$$

Here, $\varepsilon_i = n_i^2$ $(i = 1, 2, 3, 4)$, $r_{i,i+1}$ is the Fresnel reflection coefficient at the interface between layer i and layer $i+1$, and $k_{z,i}$ denotes the wave vector component normal to the interface in layer i. Note that (2) is valid even when the reflectance dip does not exactly correspond to the SPR due to the Fano resonance, as long as appropriate values of the permittivity are used.

Figure 6(a)–(c) show the calculated reflectance spectra for various thickness h_3 of the oxide layer $[Al_2O_3 + Al(OH)_3]$ in three cases of the fixed Al thickness, and the relative permittivity ε_3 of the oxide layer for each h_3 is given by (1). Figure 6(d) shows the SPR dip position extracted from the reflectance spectra as a function of h_3. The SPR dip angle decreases as h_3 decreases. Therefore, the measured shift of the SPR dip to a smaller angle observed up to 20 min may be related to the decrease in the thickness of the oxide layer, although a shift caused by the inhomogeneous covering of the NaCl solution, as seen in the case of Au, might be involved. The thickness of the oxide layer at 0 minute is estimated to be 11.4 nm from a comparison between the experimental value [Fig. 4(c)] of the dip angle 71.05° at the immersion time of 0 min and the model calculation for the Al thickness of 21 nm (TEM measurement) in Fig. 6(d). The thickness of the oxide layer at the immersion time of 20 min with the dip angle of 70.95° is estimated to be 10.7 nm. These estimations indicate that the air-formed oxide film thickness was increased in aqueous solution, which is consistent with the report by Oliveira *et al.* [11]. They reported that the thickness of the oxide increased from 4.6 nm to 12.3 nm upon contact with an aqueous solution.

Figure 7(a)–(c) show the calculated reflectance spectra for various Al thicknesses with oxide thickness h_3 as a parameter, Fig. 7(d) shows the SPR dip position as a function of the Al thickness with h_3 as a parameter. Here, relative permittivity of the oxide layer ε_3 is calculated individually for each h_3. For the Al thickness smaller than 25 nm, which correspond to the present experiment, the SPR dip angle increases as the Al thickness decreases regardless of h_3. Therefore, the increase

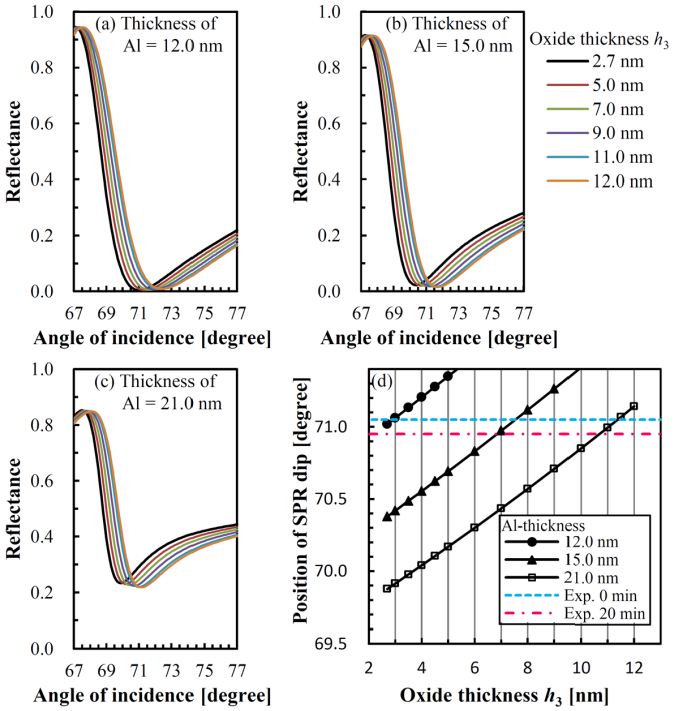

Fig. 6. (a)–(c) Calculated reflectance spectra for various oxide $[Al_2O_3 + Al(OH)_3]$ thicknesses h_3 with fixed Al thicknesses. (d) SPR dip angle extracted from (a)–(c) as functions of h_3. The dashed line shows the experimental value [Fig. 4(c)] of the SPR dip angle 71.05° (70.95°) at the immersion time of 0 min (20 min).

in the SPR dip angle observed in the experiment shown in Fig. 4(b) can be explained by the decrease in the Al thickness. By comparing with the case of $h_3 = 11.0$ nm in Fig. 7(d), the decrease in the effective Al thickness due to the corrosion can be estimated to be around 10 nm for the 20 hours of immersion.

It is possible that the oxide layer $[Al_2O_3 + Al(OH)_3]$ increases accordingly to the thinning of the Al layer. However, in the present experiment, the NaCl solution flows on the sample surface by which the corrosion products can be removed, similarly to the effect of rain in practical cases [17, p. 255]. Because it is difficult to know the actual thickness of the oxide layer, in this evaluation, we considered the case of fixed oxide thickness.

On the other hand, as seen in Fig. 7(a)–(c), with the thinning of Al, the dip becomes deep first and then gets shallow regardless of the h_3. The reflectance at the dip is determined by the balance between the material loss and the radiation loss. Here, the radiation from the surface plasmon on the NaCl-solution side of the Al film to the substrate increases exponentially, while the material loss tends to decrease, as the Al thickness decreases [30]. Zero reflectance corresponds to the balanced (critical) point. For the estimated case of $h_3 = 11.0$ nm as shown in Fig. 7(c), the dip is predicted to deepen for the change in the Al thickness (the dip angle) from 21 nm (70.95°) to 13 nm (72°) and then to shallow for the further decrease in Al thickness while the dip angle continues to increase.

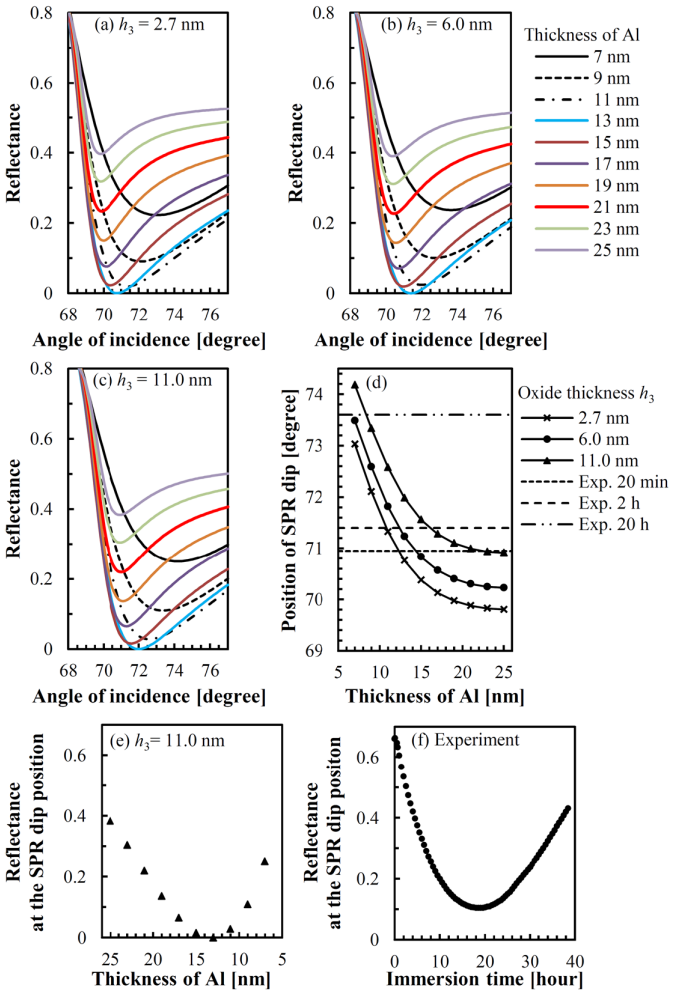

Fig. 7. (a)–(c) Calculated reflectance spectra for various Al thicknesses with fixed oxide [Al_2O_3 + $Al(OH)_3$] thicknesses h_3. (d) SPR dip position extracted from (a)–(c) as functions of Al thickness. The dashed lines correspond to the experimental value [Fig. 4(b), (c)] of the SPR dip angle 70.95°, 71.4°, and 73.6° at the immersion time of 20 min, 2 hours, and 20 hours, respectively. (e) Calculated reflectance at the SPR dip as a function of Al thickness. (f) Experimental reflectance at the SPR dip as a function of immersion time.

The measured reflectance at the dip as a function of the immersion time is compared with the predicted dip reflectance as a function of the Al thickness in Fig. 7(e) and (f). The variation observed in the experiment is qualitatively consistent with the model prediction, supporting the interpretation for the increase in the dip angle being due to the Al thinning. Experimentally, however, the dip gets shallow for the immersion time after 20 h [reflectance spectra are not shown in Fig. 4(a) for the sake of clearness], without reaching the critical point. We speculate that the scattering caused by the roughening of the film, which works effectively as additional material loss, becomes larger so that both the net material loss and the radiation loss increase for the longer corrosion time and then the critical coupling did not occur. The scattering was indeed visible on the sample surface after the immersion as long as 10 hours.

In Fig. 7(a)–(c), we can see that the SPR spectra become very broad when the Al thickness is lower than 13 nm. The main reason for this broadening is the increased radiation. The resonant width becomes large due to the increase of radiation loss of the surface plasmon, and the asymmetry of the Fano line shape is enhanced due to the interference between the increased radiation from the surface plasmon and the directly reflected wave [30].

The present calculation assuming uniform and flat layers only describes the change in effective thickness during the corrosion process. Moreover, the actual permittivity of the Al film and its oxide fabricated in this work may differ from those used in the calculation. In spite of such difficulties, the present work shows that the model calculation can fit the experimental results reasonably well. Though the estimation becomes less precise for longer immersion time as mentioned above, the corrosion is surely detectable in the first 2 hours (corresponding to the dip shift of 0.45° and the decrease in the Al thickness of 5 nm) in the case of 3 wt% NaCl solution for which the influence of the roughening might be sufficiently small, by tracing the dip position as shown in Fig. 4(c). Hence, it is concluded that the early stage of Al corrosion can be detected at the nanometer scale by utilizing SPR.

Finally, let us comment briefly on the corrosion process. On the basis of the comparison of the experimental results and the multilayer model, the possible progress of corrosion at the initial stage implies that the underlying Al only starts to corrode after the thinning of the oxide overlayer. Subsequently, the corrosion of the underlayer Al severely dominates the shift of the SPR dip position. These corrosion models are consistent with the penetration mechanism and the film thinning mechanism mentioned above. The rupturing mechanism may also present, but it cannot be directly observed in the SPR method.

IV. Conclusion

This study demonstrated the measurement of Al corrosion in 3 wt% NaCl solution utilizing SPR in the Kretschmann configuration. It was shown that the SPR measurement can detect the initial stage of Al corrosion with a change in the Al thickness in the nanoscale within a few hours of measurement. Such a rapid measurement of the corrosion is beneficial for assessing the corrosion resistance of Al-based structural and electrical components, which are expected to be used more widely in the future, the performance of anti-corrosion treatments, as well as the corrosivity of environments. Moreover, it may facilitate our understanding of the corrosion mechanism in combination with other measurement methods.

Acknowledgment

The authors would like to thank Dr. Satoka Ohnishi (Yazaki Research and Technology Center) for performing the TEM measurements of Al samples. The authors also would like to thank Tomoki Okubo (Yazaki Research and Technology Center) for performing the angle-resolved XPS measurements of Al samples.

References

[1] J. Homola, S. S. Yee, and G. Gauglitz, "Surface plasmon resonance sensors: Review," *Sens. Actuators, B: Chem.*, vol. 54, nos. 1–2, pp. 3–15, 1999.

[2] C. Nylander, B. Liedberg, and T. Lind, "Gas detection by means of surface plasmon resonance," *Sens. Actuators*, vol. 3, pp. 79–88, Jan. 1982.

[3] B. Liedberg, C. Nylander, and I. Lunström, "Surface plasmon resonance for gas detection and biosensing," *Sens. Actuators*, vol. 4, pp. 299–304, Jan. 1983.

[4] E. Kretschmann and H. Raether, "Notizen: Radiative decay of non radiative surface plasmons excited by light," *Zeitschrift für Naturforschung A*, vol. 23, no. 12, pp. 2135–2136, Dec. 1968.

[5] A. P. Vinogradov, A. V. Dorofeenko, A. A. Pukhov, and A. A. Lisyansky, "Exciting surface plasmon polaritons in the kretschmann configuration by a light beam," *Phys. Rev. B*, vol. 97, no. 23, Jun. 2018, Art. no. 235407.

[6] D. V. Nesterenko, S. Hayashi, and Z. Sekkat, "Asymmetric surface plasmon resonances revisited as fano resonances," *Phys. Rev. B, Condens. Matter*, vol. 97, no. 23, Jun. 2018, Art. no. 235437.

[7] P. R. West, S. Ishii, G. V. Naik, N. K. Emani, V. M. Shalaev, and A. Boltasseva, "Searching for better plasmonic materials," *Laser Photon. Rev.*, vol. 4, no. 6, pp. 795–808, Nov. 2010.

[8] M. W. Knight, N. S. King, L. Liu, H. O. Everitt, P. Nordlander, and N. J. Halas, "Aluminum for plasmonics," *ACS Nano*, vol. 8, iss. 1, pp. 834–840, Jan. 2014.

[9] D. Gérard and S. K. Gray, "Aluminium plasmonics," *J. Phys. D, Appl. Phys.*, vol. 48, no. 18, May 2015, Art. no. 184001.

[10] R. J. Bussjager and H. A. Macleod, "Using surface plasmon resonances to test the durability of silver–copper films," *Appl. Opt.*, vol. 35, no. 25, p. 5044, Sep. 1996.

[11] L. C. Oliveira, A. Herbster, C. da Silva Moreira, F. H. Neff, and A. M. N. Lima, "Surface plasmon resonance sensing characteristics of thin aluminum films in aqueous solution," *IEEE Sensors J.*, vol. 17, no. 19, pp. 6258–6267, Oct. 2017.

[12] E. McCafferty, *Introduction to Corrosion Science*. New York, NY, USA: Springer-Verlag, 2010.

[13] C. Leygraf, I. O. Wallinder, J. Tidblad, and T. Graedel, *Atmospheric Corrosion*, 2nd ed. Hoboken, NJ, USA: Wiley, 2016.

[14] M. C. Reboul, T. J. Warner, H. Mayer, and B. Barouk, "A ten step mechanism for the pitting corrosion of aluminium alloys," *Corrosion Rev.*, vol. 15, nos. 3–4, pp. 471–496, Jan. 1997.

[15] E. McCafferty, "Sequence of steps in the pitting of aluminum by chloride ions," *Corrosion Sci.*, vol. 45, no. 7, pp. 1421–1438, Jul. 2003.

[16] P. M. Natishan and W. E. O'Grady, "Chloride ion interactions with oxide-covered aluminum leading to pitting corrosion: A review," *J. Electrochem. Soc.*, vol. 161, no. 9, pp. C421–C432, 2014.

[17] C. Vargel, *Corrosion of Aluminium*. Amsterdam, The Netherlands: Elsevier, 2004.

[18] E. Kretschmann, "The ATR method with focused light—Application to guided waves on a grating," *Opt. Commun.*, vol. 26, no. 1, pp. 41–44, Jul. 1978.

[19] B. R. Strohmeier, "An ESCA method for determining the oxide thickness on aluminum alloys," *Surf. Interface Anal.*, vol. 15, no. 1, pp. 51–56, Jan. 1990.

[20] H. D. Ebinger and J. T. Yates, "Electron-impact-induced oxidation of Al(111) in water vapor: Relation to the cabrera-mott mechanism," *Phys. Rev. B, Condens. Matter*, vol. 57, no. 3, pp. 1976–1984, Jan. 1998.

[21] C. Langhammer, M. Schwind, B. Kasemo, and I. Zoricì, "Localized surface plasmon resonances in aluminum nanodisks," *Nano Lett.*, vol. 8, no. 5, pp. 1461–1471, May 2008.

[22] J. Evertsson *et al.*, "The thickness of native oxides on aluminum alloys and single crystals," *Appl. Surf. Sci.*, vol. 349, pp. 826–832, Sep. 2015.

[23] D. Barchiesi, "Numerical retrieval of thin aluminium layer properties from SPR experimental data," *Opt. Express*, vol. 20, no. 8, pp. 9064–9078, Apr. 2012.

[24] SIGMA KOKI. *Optics & Optical Coatings. Guide: Technical Reference*. Accessed: Dec. 2, 2019. [Online]. Available: https://www.global-optosigma.com/en_jp/category/opt_d/opt_d01.html

[25] A. D. Raki, "Algorithm for the determination of intrinsic optical constants of metal films: Application to aluminum," *Appl. Opt.*, vol. 34, no. 22, pp. 4755–4767, Aug. 1995.

[26] R. W. Revie, *Uhlig's Corrosion Handbook*, 3rd ed. Hoboken, NJ, USA: Wiley, 2011, pp. 720–729.

[27] R. Boidin, T. Halenkoviï, V. Nazabal, L. Bene, and P. Nämec, "Pulsed laser deposited alumina thin films," *Ceram. Int.*, vol. 42, no. 1, pp. 1177–1182, Jan. 2016.

[28] M. N. Polyanskiy. *Optical Constants of* Al_2O_3. Accessed: Dec. 2, 2019. [Online]. Available: https://refractiveindex.info/?shelf=main&book=Al2O3&page=Boidin

[29] W. M. Haynes, *CRC Handbook of Chemistry and Physics*, 97th ed. Boca Raton, FL, USA: CRC Press, 2016, pp. 4–135.

[30] M. Nishida, T. Matsumoto, H. Koga, T. Kosako, and Y. Kadoya, "Evaluation of surface roughness of metal films using plasmonic fano resonance in attenuated total reflection," *Phys. Rev. B*, vol. 101, no. 8, Feb. 2020, Art. no. 085414.

Terukazu Kosako received the B.E. and M.E. degrees in electrical engineering from Hiroshima University, Higashihiroshima, Japan, in 2005 and 2007, respectively, and the Doctor of Engineering degree from the Graduate School of Advanced Science of Matter, Hiroshima University in 2016.

From 2010 to 2013, he investigated metal oxide thin films in Shinoda Plasma, Company, Ltd., Japan. Since 2014, he has been a Researcher with the Yazaki Research and Technology Center, YAZAKI Corporation, Japan. His current research interests include plasmonics and corrosion of metals. He is also a member of the Japan Society of Applied Physics and the Japan Society of Corrosion Engineering.

Munehiro Nishida received the B.S., M.S., and Ph.D. degrees in physics from Waseda University, Tokyo, Japan, in 1994, 1996, and 2002, respectively.

From 2000 to 2003, he was a Research Associate with Waseda University. From 2003 to 2004, he was a Postdoctoral Fellow with Hokkaido University. Since 2004, he has been an Associate Professor with Hiroshima University. His current research interests include plasmonics, nano-optics, quantum physics, and computational physics. He is also a member of the Japan Society of Applied Physics and the Physical Society of Japan.

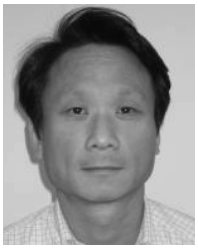

Yutaka Kadoya (Member, IEEE) received the B.E. and the M.E. degrees in electronics from Kyoto University, Kyoto, Japan, in 1984 and 1986, respectively, and the D.E. degree from the University of Tokyo, Tokyo, Japan, in 1996.

From 1986 to 1994, he investigated the compound semiconductor devices in R&D Division, Sumitomo Electric Industries, Ltd., and the Research and Development Corporation of Japan. From 1994 to 1997, he was a Research Associate with Hiroshima University. In 1998, he was appointed as an Associate Professor. Since 2004, he has been a Professor with Hiroshima University. His current research interests include terahertz-wave technology and science, optical meta-materials, and plasmonics. He is a member of the Japan Society of Applied Physics, the Laser Society of Japan, and the Optical Society of America.